The Straight-Chain Segment Length Distribution in Xerogels of UHMWPE, Which Provide High Drawability of Gel-Derived Fibers

P. Pakhomov,[1] V. Galitsyn,[2] Svetlana Khizhnyak,[1] A. Tshmel[3]

[1]*Physico-Chemistry Department, Tver' State University, 170002 Tver', Russia*
[2]*Institute of Synthetic Fiber, 170032 Tver', Russia*
[3]*Fracture Physics Department, Ioffe Physico-Technical Institute, Russian Academy of Sciences, 194021 St. Petersburg, Russia*

Received 26 September 2006; accepted 30 March 2007
DOI 10.1002/app.26543
Published online 16 May 2007 in Wiley InterScience (www.interscience.wiley.com).

ABSTRACT: A series of ultra-high-molecular-weight reactor powders with different technological prehistory were utilized for obtaining fibers through the gel technology. The fibers prepared from some powders exhibited high draw ratios and good mechanical properties (Young's modulus and tensile stress) but other powders yielded fibers of very low drawability. The low-frequency Raman study revealed that the straight-chain-segment (SCS) length distributions in dried gels prepared from powders of ''drawable'' group are bimodal, while the gels issued from powders unsuitable for fiber drawing have unimodal length distributions of SCS. © 2007 Wiley Periodicals, Inc. J Appl Polym Sci 105: 2984–2987, 2007

Key words: gels; polyethylene; Raman spectroscopy; strength

INTRODUCTION

The performance of the polyethylene (PE) fibers obtained through the gel technology is determined by the properties of the tenuous network of molecular entanglements in gels, which should promote a highly regular arrangement of polymer chains at the stage of fiber drawing. However, even the network with optimal amount of entanglements cannot be transformed to the ordered structure if the entanglements are too durable. According to De Gennes[1] and Keller,[2] the molecular entanglements in polymer gels are realized by small crystallites that serve as fixation elements. The crystalline nature of the chain fixers in PE gels was supported by the IR and Raman spectroscopic studies.[3]

In this light, the properties of crystallites in gelled polymer could determine, to some extent, the capability of the given gel solution to yield high performance fibers after a routine drawing process. In this communication, the characteristics of crystalline substance in a series of xerogels obtained from the powders of ultra-high-molecular-weight PE (UHMW PE) with different technological prehistory were studied with the help of the low-frequency Raman spectroscopy, which provides the information on the length distribution of straight chain segments (SCS) in linear polymers. The gelled powders were also used for drawing fibers with maximum achievable draw ratio (DR). Our goal was to find a correlation between the parameters of crystallites in gels and the drawability of gel-derived fibers.

EXPERIMENTAL

Samples

The reactor powders were prepared using different modifications of the supported titan-magnesium catalyst obtained in the Boreskov Institute of Catalysis (Novosibirsk). The molecular weight (MW) and the polymerization temperature (T_{poly}) of the reactor powders are given in Table I.

Fibers were formed from gel solution at 172°C. The flow from a multihole die was directed into a bath filled with a paraffin oil at 25°C. The formed fiber was subjected to preliminary stretching at 74°C. Then the fiber was arranged in a container for 20 h during which it shrank to $\sim$ 0.6 of its initial length. Finally, the samples were drawn to their final DR in an oil paraffin bath heated to 130°C.

The xerogels needed for the Raman spectroscopic analysis were obtained by washing the gels in hexane (6 times during 1 h in each cycle) with subsequent drying of washed gels during 4 h at temperature 50°C.

Correspondence to: A. Tshmel (alex@ac7773.spb.edu).
Contract grant sponsor: the Russian Foundation of Basic Research; contract grant numbers: 06-03-32609a, 06-03-08111ofi.

TABLE I
Characteristics of Original Reactor Powders and Gel-Derived Fibers

	Powder		Fiber		
Sample	M_W[a] × 10^6	T_{poly} (°C)	λ_{max}	E (GPa)	σ (GPa)
A	1.2	60	54	89	3.1
B	2.0	60	53	98	2.9
C	2.4	50	46	104	3.3
D	3.4	55	29	89	2.7
E	2.0	70	Cannot be drawn	–	–
F	2.5	60	Cannot be drawn	–	–

[a] Viscosity-average molecular weight.

Mechanical tests

The mechanical tests were performed on 150 mm pieces of samples with the help of the Instron 1122 machine operating in the tensile mode. Strain rate of tests was 50 mm/s; the Young's module (E) was measured at 2% level of strain. The maximum achieved DRs (λ_{max}), E, and tensile strength (σ) of the fibers are given in Table I. One can see that all samples can be divided into two groups in accordance with their drawability: a ''normal'' group of fibers whose DR was more than 30, and an ''undrawing'' group, which was inappropriate for fiber production.

Raman measurements

The Raman spectra of dried gels were measured in the 90° geometry on a triple monochromator Spex Model 1401 equipped with a 50 mW He-Ne laser.

The measurements were carried out in the spectral range 5–60 cm^{-1} where the bands belonging to longitudinal acoustic modes (LAM) propagating along the all-trans sequences appear. The shape of such LAM band is determined by the actual set of all-trans sequences, that is by the SCS length distribution.

The LAM band in the low-frequency Raman spectrum is insensitive to the localization of the SCS in either crystalline or amorphous regions, since the acoustic vibrations of this kind are excited in individual macromolecules, and their frequency, in fact, does not depend the nature of the chain environment.

Length of the ordered (all-trans) sequence, L, and LAM frequency, v_L, are related as

$$L = (2cv_L)^{-1} \times (E/\rho)^{1/2} \quad (1)$$

where c is the speed of light; ρ is the density, and E is the chain Young's modulus.

The SCS length distribution function, $F(L)$, depends not only on the number of vibrating SCS but also on the scattering efficiency of light and the population of vibrational energy levels:[4]

$$F(L) \propto [1 - \exp(-\mathrm{hcv/kT})]v^2 I$$

Here h is Plank's constant, k is Boltzmann's constant, T is the absolute temperature and I is the Raman intensity. The expression in brackets characterizes the Boltzmann population of vibrational energy levels. The value of distribution function at given L is proportional to the fraction amount of the SCS with the length equal to L. The details of the data processing were given previously.[5]

The original Raman spectra and the SCS length distributions calculated from these spectra are depicted in Figures 1 and 2. To facilitate a comparison of samples relevant to fibers of different draw-

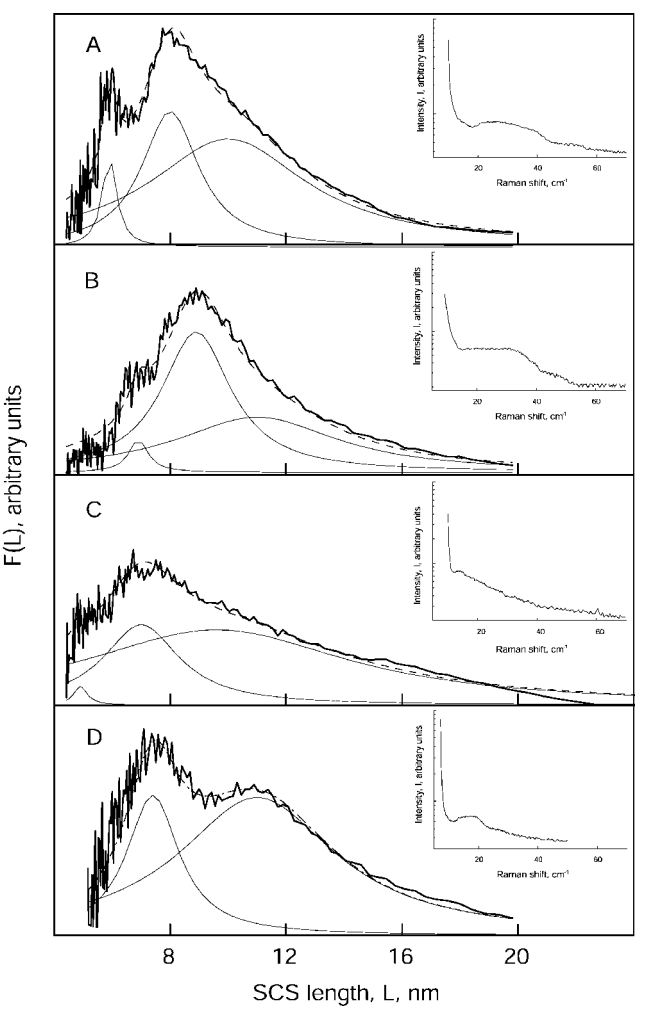

Figure 1 Raman spectra of dried gels and SCS length distributions calculated from these spectra. A logarithmic scale for the Raman intensity is chosen to represent in detail weak signals. The lettering denotes samples A–D characterized in Table I. Thin solid lines and dashed lines are Lorentz components and integrating function, respectively.

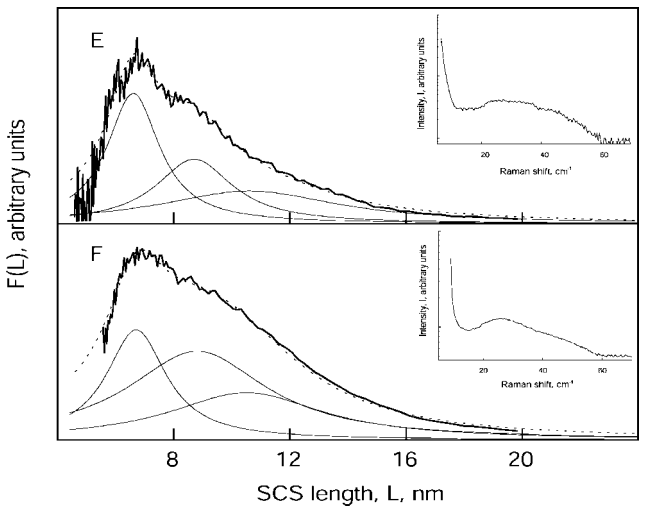

Figure 2 Raman spectra of dried gels and SCS length distributions calculated from these spectra. The lettering denotes samples E–F characterized in Table I.

ability, the Raman data are also divided into two groups in accordance with the classification given in Table I. One can see that the samples A–D belonging to the ''normal'' group exhibit bimodal SCS distributions (Fig. 1) with main peaks in the range 8–11 nm supplemented with small-amplitude features at $\sim$ 7 nm. To characterize the SCS in more detail, the profiles $F(L)$ were convoluted into a set of Lorentz components. One can see in Figure 1 that the curves A-C were successfully fitted by three components, while a two component approximation was sufficient to describe adequately the curve D. The short-length peaks (that is those situated at 6–7 nm) in all these bimodal distributions were fitted with single Lorentzians - in contrast to their asymmetric counterparts, for which only two-component fitting was successful (with the exception of the sample D). Bearing in mind the formalistic nature of the multi-component decomposition of asymmetric contours, we regard all the SCS length distributions presented in Figure 1 as bimodal in accordance with their visual aspect.

The ''nondrawable'' samples E-F have asymmetric SCS distributions with dominant peaks at 6.6 nm and ill-pronounced features situated at their right-hand wings (Fig. 2). The convolution procedure reveals high-amplitude peaks at 6.6 nm and wide-width peaks at 9–11 nm.

Thus, two SCS fractions specified by their characteristic lengths ($\sim$ 6.5 and 10 nm) manifested themselves in all samples but their relative contribution to the whole ensemble of all-trans sequences is quite different in groups A–C and E–F; the sample D exhibits intermediate properties, which will be commented in the next Section.

DISCUSSION

A direct comparison of the drawability of gel-derived fibers originated from different reactor powders reveals a persistent trend: ''normal'' fibers originate only from the gels with bimodal distribution functions (A–D); the gels E–F with the unimodal distribution function $F(L)$ were inappropriate for forming and drawing fibers. These two kinds of distributions indicate the existence of alternative structures of crystalline phase in studied gels.

Keller[2] considered a competition of folded-chain crystals (FCC) and multi-chain crystallites in gelled polymers. The molecular network bound by uniform FCC must be quite stable system, which would resist to mechanical transformation to oriented structure in the course of the extrusion process. The unimodal SCS length distributions in samples E-F evidence the prevailing contribution of the FCC fraction to the crystalline phase: their prominent peaks are described by single, narrow Lorentz components. This circumstance points out the highly regular organization of crystallites, to which the corresponded SCS belong. According to Fakirov,[6] the most favorable structure for the achievement of high DR is the crystalline phase consisting of imperfect crystallites. We suppose that it is the high strength of crystalline fixers made of FCC that hindered the drawability of gel-derived polymer in samples E and F where the FCC fraction is prevailing.

The peak shoulders represented by combinations of wide-width Lorentz components, can belong to either nonfolded crystallites or individual SCS, or both. The complicated SCS length distribution is a hallmark of the nonuniform structure of crystalline entities in gels.

The positions of small-amplitude peaks in the SCS length distributions in ''drawable'' samples coincide with the main peak positions in unimodal distributions in samples E-F. In addition, the short-length peaks in samples A–D are well-fitted with the single-component Lorentzians. Therefore, one can think that the 6–7 nm thick crystalline entities in bimodal samples have the FCC structure. The high-amplitude peaks in the samples A–D we assign to non-FCC structures characterized by the wide SCS length distribution typical for multi-chain crystals. The crystalline phase of this kind could either originate from remnant, elongated components of the source powder, such as fibrils and grain-linking bundles of SCS, or to be a result of multi-center recrystallization in gel solutions of some powders. In any case, the molecular fixers of nonfolded-chain crystals should have lower strength, and an easy uncoupling of chains in the extruder die provide optimal conditions for the rearrangement of macromolecules to regular structure.

The negative role of the FCC-organization of the gel network in forming the future mechanical properties of gel-derived fibers is confirmed indirectly by the comparison of the SCS length distribution in the sample D with its tensile strength. The bimodal profile of the function $F(L)$ evidences the presence of approximately equal FCC and non-FCC crystalline phases. Correspondingly, the sample D was drawable (due to the substantial fraction of nonfolded SCS) but the strength of the fiber prepared from this gel occurred to be lower than the strength of other ''bimodal'' gels (due to the great amount of strong molecular fixers made of FCC). In addition, one should take into account that the MW of the sample D is significantly higher than all other samples (Table I). In contrast to tensile drawing of melt-crystallized UHMW PEs whose ability to be oriented is greatly restricted by the highly developed interfibrillar phase,[7] the increase of the MW plays a positive role in the drawability of solution-crystallized UHMW PEs and polypropylenes.[8,9] Therefore, the sample D could be more drawable than the samples E and F despite a substantial contribution of FCC to its SCS length distribution. Correspondingly, the mechanical properties of the sample D are comparable with those of samples A–C despite its relatively low DR. Uehara et al.[9] observed a similar effect and explained it by the small amount of chain ends in the highest-MW reactor powders.

Interestingly, the drawability of the gels A-C decreases from 54 to 46 with the twofold MW increase, while the Young's modulus simultaneously grows from 89 to 104 GPa. One can think that in addition to a reduced amount of chain ends, the MW increase causes the formation of more connected gel network; this hinders the drawability but enhances the structural rigidity of oriented polymer.

There is a variety of molecular and supermolecular parameters that govern the properties of gel-derived polymer products. The most important factors that determine the polymer drawability are the MW[8,9] and the morphology of powder particles.[9–13] This work confirms the significance of the polymer MW and demonstrates that the nature of crystalline fixers in the gel network affects the efficiency of gel-to-fiber transformation to a noticeable extent. In future, we hope to bind the presented here results with the morphological patterns of used reactor powders, thus covering different aspects of the problem (molecular, morphological, and structural) in a common series of experiments.

Finally, when considering the presented results, one should bear in mind that the experiments were performed on dried gels, which are more appropriate for the Raman measurements than gel solutions (due to high level of parasitic scattering in latter substances). The release of the solvent could affect to some extent the crystalline structure of gels; however, the qualitative changes are low probable under applied drying procedure.

CONCLUSIONS

The length distributions of SCS were calculated from the low-frequency Raman spectra to assess the perfection of crystalline entities in UHMWPE gels. The crystallites in polymer gels play a role of fixers of macromolecules needed to form the molecular network, and the amount and strength of the fixers determines a capability of the network to be transformed to regular oriented structure during the drawing process. It was found in this study that the UHMWPE gels with the crystalline phase consisting mainly of small size (6–7 nm), uniform crystals (suggested FCC) are not suitable for manufacturing oriented fibers in contrast to gels with crystalline fixers built of multi-chain crystals. We suppose that high durability of perfect crystallites hinders rupturing of the molecular network needed for regular chain arrangement. The fixers in gels with structurally complicated, heterogeneous crystalline phase are not stable under the action of mechanical force, and transform readily into ordered structure when being subjected to the extrusion procedure.

References

1. De Gennes, P.-G. Scaling Concepts in Polymer Physics; Cornell University Press: Ithaca, NY, 1978.
2. Keller, A. Faraday Discuss. 1995, 101, 1.
3. Pakhomov, P. M.; Khizhnyak, S.; Reuter, H.; Lechner, M.; Tshmel, A. Macromolecules 2003, 36, 4868.
4. Snyder, R. G.; Krause, S. J.; Scherer, J. R. J Polym Sci Phys Ed 1978, 16, 1593.
5. Pakhomov, P. M.; Khizhnyak, S.; Reuter, H.; Galitsyn, V.; Tshmel, A. Polymer 2003, 44, 4651.
6. Fakirov, S. Oriented Polymer Materials. Hüthry, S. F.; Heidelberg, W. Verlag: Oxford, USA, 1996, pp 422–443, .
7. Marikhin, V. A.; Myasnikova, L. P.; ibid, pp 38–98, .
8. Wang, L. H.; Ottani, S.; Porter, R. S. Polymer 1991, 32, 1776.
9. Uehara, H.; Hirao, T.; Yamanobe, T.; Komoto, T.; Yamamoto, Y. Polymer 2006, 47, 7145.
10. Kanamoto, T.; Ohama, T.; Tanaka, R.; Takada, M. Polymer 1987, 28, 1517.
11. Truss, R. W.; Han, K. S.; Wallace, J. F.; Geil, P. H. Polym Eng Sci 1980, 20, 747.
12. Han, K. S.; Wallace, J. F.; Truss, R. W.; Geil, P. H. J Macromol Sci Phys B 1981, 19, 313.
13. Ivan'kova, E. M.; Myasnikova, L. P.; Marikhin, V. A.; Baulin, A. A.; Volchek, B. Z. J Macromol Sci Phys B 2001, 40, 813.